

**Distribution Agreement**

In presenting this thesis as a partial fulfillment of the requirements for a degree from Emory University, I hereby grant to Emory University and its agents the non-exclusive license to archive, make accessible, and display my thesis in whole or in part in all forms of media, now or hereafter known, including display on the World Wide Web. I understand that I may select some access restrictions as part of the online submission of this thesis. I retain all ownership rights to the copyright of the thesis. I also retain the right to use in future works (such as articles or books) all or part of this thesis.

Signature:

---

Fu Wei Pang

April 16, 2013  
Date

Effects of stress on A-type K<sup>+</sup> channel subunit Kv4.2 distribution in the basolateral amygdala

By

Fu Wei Pang

Adviser

E. Christopher Muly, MD, PhD

Neuroscience and Behavioral Biology Program

---

E. Christopher Muly, MD, PhD  
Adviser

---

Paul R. Lennard, PhD  
Committee Member

---

Yoland Smith, PhD  
Committee Member

April 16, 2013  
Date

Effects of stress on A-type K<sup>+</sup> channel subunit Kv4.2 distribution in the basolateral amygdala

By

Fu Wei Pang

Adviser

E. Christopher Muly, MD, PhD

An abstract of  
A thesis submitted to the Faculty of Emory College of Arts and Sciences  
of Emory University in partial fulfillment  
of the requirements of the degree of  
Bachelor of Sciences with Honors

Program in Neuroscience and Behavioral Biology

2013

## Abstract

Effects of stress on A-type K<sup>+</sup> channel subunit Kv4.2 distribution in the basolateral amygdala

By Fu Wei Pang

Potassium channels make up the largest and most diverse class of voltage-gated ion channels in the nervous system. Voltage-gated A-type K<sup>+</sup> (Kv) channel subunit Kv4.2 modulates dendritic excitability and synaptic plasticity. As such, voltage-gated channels like Kv4.2 are partially involved in the formation of memory. The basolateral amygdala (BLA) is a recognized locus for pairing of stimuli during fear conditioning. However, little is known about the distribution and function of Kv4.2 in the BLA. Therefore, does Kv4.2 play a role in stress-mediated plasticity in the BLA? We used immunohistochemical techniques at the electron microscopic level to determine the normal distribution of voltage-gated potassium channel subunit Kv4.2 in rat BLA neurons. Additionally, we showed that there was a stress-mediated increase in Kv4.2 localization in dendritic spines. These results suggest a possible compensatory mechanism to decrease pathologic dendritic excitability observed in patients with fear and anxiety disorders.

Effects of stress on A-type K<sup>+</sup> channel subunit Kv4.2 distribution in the basolateral amygdala

By

Fu Wei Pang

Adviser

E. Christopher Muly, MD, PhD

A thesis submitted to the Faculty of Emory College of Arts and Sciences  
of Emory University in partial fulfillment  
of the requirements of the degree of  
Bachelor of Sciences with Honors

Program in Neuroscience and Behavioral Biology

2013

## Acknowledgements

I would like to thank Marcelia Maddox for technical assistance with the immunohistochemical experiments. This work was supported by a Merit Award from the Office of Research and Development, Department of Veterans Affairs to ECM; by NIMH grant MH069852 to DGR; and by an NIH/NCRR base grant [Grant P51RR000165] to Yerkes National Primate Research Center.

## **TABLE OF CONTENTS**

LIST OF FIGURES	i
INTRODUCTION	1
MATERIALS & METHODS	4
RESULTS	10
DISCUSSION	16
REFERENCES	23

**LIST OF FIGURES**

<i>Figure. 1: Intracellular localization of Kv4.2</i>	28
<i>Figure. 2: Subcellular localization of Kv4.2 in the BLA</i>	29, 30
<i>Figure. 3: Effect of stress on Kv4.2 distribution</i>	31
<i>Figure. 4: No significant reduction in putative interneuron dendritic labeling</i>	32

## 1. Introduction

The action potential (AP) is an electrical signal generated in neurons due to changes in membrane permeability to specific ions (Purves *et al.*, 2008). An AP arises from a voltage-dependent rapid, transient rise in sodium ion ( $\text{Na}^+$ ) permeability, followed by a delayed and prolonged rise in potassium ion ( $\text{K}^+$ ) permeability. The *Shal*-type channel (Kv4.x) is a family of voltage-gated potassium channels highly expressed in brain tissue. It contributes to the transient (A-type), voltage-dependent  $\text{K}^+$  currents ( $I_A$ ) involved in the AP (Birnbaum *et al.*, 2003). This  $I_A$  current is responsible for repolarization of the neuron and tends to reduce depolarization. The Kv4.x family of proteins is pore-forming and voltage-sensing  $\alpha$  subunits that join into homo- or hetero-tetramer configurations (Trimmer & Rhodes, 2004; Menegola *et al.*, 2008). The mammalian *Shal*-type group of potassium channels are comprised of three different  $\alpha$  subunits: Kv4.1, Kv4.2 and Kv4.3. Previous studies have demonstrated that these  $\alpha$  subunits activate in response to membrane depolarization, rapidly inactivating and recovering quickly from inactivation in comparison to other Kv channels (Birnbaum *et al.*, 2003).

Of particular interest is protein subunit Kv4.2. *In vitro* studies have suggested that Kv4.2 channels are located in the plasma membrane of dendritic shafts and spines of neurons (Jensen *et al.*, 2011). Additional *in vivo* studies of Kv4.2 have been largely focused on hippocampal CA1 neurons where results have also supported previous *in vitro* findings of dendritic expression of Kv4.2 (Sheng *et al.*, 1995; Hoffman *et al.*, 1997; Kim *et al.*, 2007; Menegola *et al.*, 2008). These studies have found a non-uniform distribution of Kv4.2, with highest expression levels in distal dendrites (Hoffman *et al.*, 1997). Chemical loss-of-function studies, using Hetropodatoxin3 (HpTX3), a selective Kv4

channel blocker, revealed an elimination of A-type  $K^+$  currents in dendritic hippocampal CA1 neurons (Ramakers & Storm, 2002). A more specific genetic loss-of-function study using Kv4.2 knockout mice also demonstrated the same effect (Chen *et al.*, 2006). This loss of A-type  $K^+$  currents resulted in an increase in the amplitude of dendritic back-propagating action potentials (bAPs), lowering the threshold for induction of long-term potentiation (LTP) (Chen *et al.*, 2006). These studies suggest Kv4.2 as a modulator of bAPs and specific forms of synaptic plasticity. Further studies by Kim *et al.* found a NMDAR- and  $Ca^{2+}$ - dependent regulation and redistribution of Kv4.2, with AMPAR activation alone insufficient to trigger this change (Kim *et al.*, 2007). Alterations in Kv4.2 expression between dendrites and spines affect the amplitude and charge of mini excitatory postsynaptic current (mEPSC) recorded in the soma (Hoffman *et al.*, 1997). Through the internalization of Kv4.2 in active spines, mEPSC efficacy is enhanced through a NMDAR- and  $Ca^{2+}$ -dependent mechanism, lowering the threshold for induction of LTP (Kim *et al.*, 2007). This finding suggests an additional mechanism for synaptic plasticity and fine-tuning of dendritic signaling. Therefore, these studies suggest that protein channel Kv4.2 regulates dendritic excitability, modulating the action potential's duration and frequency.

Although most of Kv4.2 physiology has been studied in the hippocampus, recent studies have begun to explore its distribution and function in other brain regions. Brain regions with high Kv4.2 expression levels, such as the bed nucleus of the stria terminalis (BNST) and intercalated cell clusters (ITCs) within the amygdala nuclei, are also associated in stress and emotional processing (Lockridge *et al.*, 2010; Kaufmann *et al.*,

2012; Rannie *et al.*, submitted). This raises the question, does Kv4.2 play a role in emotional processing and stress mediated plasticity?

Response to fear and stress is a hardwired process involving the amygdala (Davis, 1992). Behavioral studies have suggested that the BLA is involved in conditioning and assigning emotional significance to sensory stimuli (Davis *et al.*, 1994; Nader *et al.*, 2001; Walker & Davis, 2008). It receives inputs from the sensory cortex, thalamus and hippocampus, integrating multiple streams of information (Davis *et al.*, 1994; McDonald, 1998). The BLA then sends out glutamatergic projections to other brain regions involved in anxiety and fear, including the central nucleus of the amygdala (CeA) and the BNST (Davis *et al.*, 1994; McDonald, 1998). Therefore, because the BLA receives multiple inputs from different brain regions, it can act as a substrate for sensory convergence, and is considered a recognized locus for pairing of stimuli during fear conditioning (Maren *et al.*, 1996). Previous electrophysiological studies have demonstrated plastic changes in physiological properties, specifically modification of AMPA receptors, in response to stress in the BLA (Walker & Davis, 2008). Furthermore, studies have shown that inactivation of the BLA during learning through pharmacological intervention abolishes acquisition of fear conditioning (Muller *et al.*, 1997, Helmstetter & Bellgowan, 1994).

Imaging studies of patients with anxiety disorders suggest higher amygdala basal activity levels (Etkin & Wager, 2007; Rabinak *et al.*, 2011), in addition to heightened amygdala activity to fear-inducing stimuli compared to controls (Rauch & Shin, 1997; Rauch *et al.*, 2006; Shin & Liberzon, 2010; Linnman *et al.*, 2011). Extreme traumatic events have also been shown to enhance memory formation (Shors, 2001; McGaugh & Roozendaal, 2002). Functional magnetic resonance imaging (fMRI) studies of patients

suffering from posttraumatic stress disorder (PTSD) have also demonstrated increased amygdala activity to neutral stimuli, indicating an abnormal amygdala response to non-threatening conditions (Brunetti *et al.*, 2010). Therefore, during stressful events, neuronal activity in the BLA might become augmented in the process of fear conditioning.

Current work in our laboratory shows that stress can modulate the localization of signaling proteins between dendrites and spines in the BLA, and in doing so, alter the response properties of the principle neurons (Hubert *et al.*, in press). Given the findings that changing Kv4.2 localization in spines is a mechanism of synaptic plasticity and that stress can change the localization of other signaling proteins in the spines of the BLA it will be important to see if Kv4.2 plays a role in stress mediated plasticity in the BLA. My first aim is to describe the distribution and function of Kv4.2 in rat BLA. My second aim is to determine whether stress causes alterations in the distribution of the voltage-gated A-type K<sup>+</sup> channel subunit Kv4.2 in the BLA.

## **2. Materials and Methods**

**Animals:** All experimental protocols strictly conformed to National Institutes of Health guidelines for the Care and Use of Laboratory Animals, and were approved by the Institutional Animal Care and Use Committees of the Atlanta VA and Emory University. For immunohistochemical experiments we used 23 adult, male, Sprague–Dawley rats that were 43 days old at the beginning of the first footshock session (Charles River, Wilmington, MA, USA).

For our stress studies, we used a repeated unpredictable foot shock protocol (Hazra *et al.*, 2012). Here, rats receiving shock stress were placed in a testing chamber

(Lafayette Instruments) and exposed to 16 randomly timed foot shocks during a 30 minute period and then returned to their home cages. The shocks were 0.5mA and lasted for 0.5s, and the half-hour session was broken down into a 5-minute habituation session followed by three eight-minute periods. Rats received eight random shocks in the first and third eight-minute periods. Rats underwent this shock protocol daily for four days. All rats were 43 days old on the first stress day, and age-matched control groups remained in home cages without shocks.

Stressed rats and their age-matched controls were sacrificed at either one or six days following the final day of the footshock protocol. For the immunohistochemical studies, rats were given an injection of pentobarbital (100 mg/kg i.p.), and within minutes of loss of tail-pinch reflex, transcardially perfused with at least 100 ml of cold, oxygenated Ringer's solution. This was followed by perfusion with 500 ml of fixative containing 4.0% paraformaldehyde and 0.1% glutaraldehyde, in phosphate buffer (PB, 0.1 M, pH 7.4). Brains were removed from the skull and stored overnight in 4.0% paraformaldehyde overnight at 4°C. The brains were then rinsed in phosphate-buffered saline (PBS) and cut into 60 µm-thick coronal sections on a vibratome. In order to improve penetration of immunolabeling, a freeze thaw protocol was used. Sections were transferred to a cryoprotectant solution (PB, 0.05 M, pH 7.4 containing 25% sucrose and 10% glycerol) for 20 min. They were then frozen in a -80 °C freezer for 20 min, returned to a decreasing gradient of cryoprotectant solutions and rinsed in PBS. Sections then underwent immunohistochemical procedures for the immunoperoxidase localization of Kv4.2.

## **Immunohistochemical Experiments**

Immunohistochemistry and preparation for electron microscopy was done according to standard techniques (Muly *et al.*, 2010). We used an affinity purified mouse monoclonal antibody directed against amino acids 209-225 from rat Kv4.2 (NeuroMab, Davis, CA, used at 1:1000). Specificity of the antibody has been confirmed by Western blotting, with the antisera recognizing a single band on immunoblots with a molecular weight of 75-80 kDa in rat brain and wild type mouse brain, but not Kv4.2 knockout mouse brain. In addition, no cross reactivity against rat Kv4.3 was observed (data available from NeuroMab). After immunolabeling, the sections were postfixated in 1% osmium tetroxide, dehydrated in ethanol and placed in uranyl acetate to increase contrast for the electron microscope. The sections were embedded in epoxy resin (Durcupan, Sigma-Aldrich, St. Louis, MO) and following hardening, blocks of the BLA were prepared and ultrathin sections collected and stained with lead citrate. The region of the BLA sampled was in the middle to slightly rostral region of the BLA (bregma -2.1 to -3.6) and dorsoventrally in the middle of the nucleus with a bias toward the basal half.

Forty-six blocks (2 block/animal) of BLA tissue immunostained for Kv4.2 were taken from the slides and glued on the top of resin blocks with cyanoacrylate glue. They were cut into 55-nm ultrathin sections with an ultramicrotome (Ultracut T2, Leica, Nussloch, Germany) and serially collected on single-slot Pioloform-coated copper grids. The sections were stained with lead citrate for 5 minutes (Reynolds, 1963) and examined with a JEOL 1011 electron microscope (JEOL; Munchen, Germany).

### **Single-Label Immunogold Localization of Kv4.2**

In order to validate the accuracy of DAB label, immunogold labeling was also conducted to determine the precise location of Kv4.2. Tissue from two adult rats was used for the immunogold localization of Kv4.2. Sections at the level of the BLA from two of these rats were processed for the localization of Kv4.2. Sections processed for pre-embedding immunogold were transferred to the cryoprotectant solution and frozen at  $-80^{\circ}\text{C}$  in the same way as those processed for immunoperoxidase. They were then preincubated in PBS solution containing 5% milk for 30 mins. Next, they were rinsed three times in a TBS-Gelatin (0.1% fish gelatin) solution for 3 mins at room temperature (RT) before being transferred to a TBS-Gelatin solution containing 1% milk and the primary antibody for Kv4.2 (0.98 mg/ml) for overnight incubation at RT. Next, they were rinsed three times in TBS-Gelatin for 10 mins and incubated for 2 hours in the secondary 1.4-nm gold-conjugated goat anti-mouse IgGs (Nanogold, Nanoprobes, Stonybrook, NY) at a concentration of 1:100 in 1% NGS in TBS-Gelatin solution. They were then rinsed twice in TBS-Gelatin for 10 mins, followed by two 5 min rinses of 2% aqueous Acetate buffer solution. After the Acetate buffer wash, the sections were then taken to the dark room for silver intensification of gold particles for 5–10 minutes using the HQ silver kit (Nanoprobes). They were then rinsed with PB, treated with 0.5% osmium tetroxide for 10 minutes, and dehydrated in 50% ethanol, 70% ethanol / 1% uranyl acetate for 10 mins, and then dehydrated in a graded series of alcohol and propylene oxide. The remainder of the tissue preparation was the same as that described above for the immunoperoxidase material.

Four blocks (2 blocks/animal) of BLA tissue immunostained for Kv4.2 were taken from the slides and glued on the top of resin blocks with cyanoacrylate glue. They were cut into 55-nm ultrathin sections with an ultramicrotome (Ultracut T2, Leica, Nussloch, Germany) and serially collected on single-slot Pioloform-coated copper grids. The sections were stained with lead citrate for 5 minutes (Reynolds, 1963) and examined with a JEOL 1011 electron microscope (JEOL; Munchen, Germany).

In immunogold-labeled sections from rat BLA tissue, a minimum of three gold particles was used as an arbitrary criterion to categorize dendrites as immunoreactive. Gold particles were designated as plasma membrane-bound if they were apposed to the plasma membrane. Plasma membrane-bound particles were also characterized as either being on the intracellular surface or extracellular surface of the membrane. All other gold particles were categorized as intracellular. Although many of these intracellular particles were clearly apposed to the membrane of various organelles, the ultrastructural features of these intracellular elements were often damaged. We therefore considered these gold particles as intracellular, but did not attempt to characterize the specific intracellular compartment with which they were associated. No attempt was made to categorize the axonal or glial labeling as plasma membrane-bound or intracellular because of the limited spatial resolution of large silver-intensified gold particles in small elements.

### **Tissue Data Analysis**

The grids were examined with a JEOL 1011 electron microscope (JEOL; Munchen, Germany). The immunoperoxidase labeling for Kv4.2 penetrated deep into the tissue, so we were able to sample material away from the tissue–resin interface. We randomly

selected fields of immunoreactive elements from the blocks, and images were taken at a magnification of  $\times 40,000$  using a Gatan 785 camera and examined using Gatan Digital Micrograph software (Gatan, Inc.; Pleasanton CA). Data were collected in two blocks from each stressed and control animals. In total, 23 animals were examined. The counting method used was semi-quantitative because of a subjective judgment that had to be made regarding the threshold for considering a profile as positive for a specific stain. These judgments were made based on the following criterion. On each micrograph, DAB-labeled profiles were identified based on their content of patches of DAB reaction product, darker than any adjacent mitochondria, without sharp borders suggesting crystalline deposits and contained within a membrane bound element and not appearing to overlay multiple profiles. These labeled profiles were classified as spines, dendritic shafts, terminals, axons, or glia based on ultrastructural criteria (Peters, 1991). Although the presence of DAB within the elements complicates their identification, whenever possible both the presence and the absence of multiple criteria were used to make each determination (Muly *et al.*, 2003). In cases that strong DAB, ultrastructural flaws, or absence of clear features, made ultrastructural identification difficult, the profile was discarded. Profiles were identified as spines based on size ( $0.3\text{--}1.5\mu\text{m}$  in diameter), presence of spine apparatus, absence of mitochondria or microtubules, and in some cases presence of asymmetric synaptic contacts. Dendritic shafts were identified by their greater size ( $0.5\mu\text{m}$  or more in diameter) and the presence of microtubules, mitochondria, and in some cases synaptic contacts. Axon terminals were characterized by the presence of numerous vesicles, mitochondria, and occasionally a presynaptic specialization. Preterminal, unmyelinated axons were identified by their small size ( $0.1\text{--}0.3\mu\text{m}$  in

diameter); regular, round shape; and occasional presence of synaptic vesicles or neurofilaments. Glial profiles were identified based on their characteristic shape, which appears to fill in the space between other, nearby profiles, and a relatively clear cytoplasm, which occasionally contained numerous filaments. This was a blind study where scoping and analysis were conducted without the knowledge of treatment group. The numbers of profiles immunoreactive for Kv4.2 were tabulated and the distributions compared with an ANOVA.

### **Statistics**

For the neuroanatomical studies, the total number of immunoreactive profiles (spines; dendritic shafts; terminals; axons; glia) sampled was summed for each animal. Next, the percentage of each profile was calculated by dividing the sum of each individual profile by the total number of labeled elements quantified for that animal. The groups were then compared using a 2-way ANOVA with age and labeled profiles as factors. A secondary analysis was also conducted on immunoreactive terminals. The percentage of terminals forming symmetric or asymmetric contacts was quantified, in addition to the type of postsynaptic structure it made contact with (spine; dendritic shaft). Pairwise comparisons were performed using post-hoc Scheffe tests. All data are expressed as the mean  $\pm$  SEM. A  $p < 0.05$  was considered statistically significant for all cases.

## **3. Results**

### **Intracellular Localization of Kv4.2**

In order to determine the localization of the voltage-gated A-type K<sup>+</sup> channel subunit Kv4.2 in the BLA, immunoperoxidase staining was used to reveal its location. Because

the antibody we used was predicted to bind to an extracellular S1-S2 epitope (data available from NeuroMab), it raised a potential problem for the use of immunoperoxidase labeling to reveal the ultrastructural location of this protein. If the label were indeed, outside the plasma membrane, the precise localization of Kv4.2 would be difficult to determine because the DAB label used for immunoperoxidase staining can diffuse from the site of production. Hence, to validate the accuracy of DAB label, immunogold labeling was also conducted to determine the precise location of Kv4.2, and to establish if the localization pattern is similar between labels. We found that the labeling pattern produced by immunoperoxidase and immunogold labeling was similar (Fig. 1B & C). Both produced predominately intracellular immunoreactivity (Fig.1). When the labeling was associated with the plasma membrane, it was usually found on its intracellular surface. In particular, we did not observe populations of profiles labeled by gold along the external surface of their plasma membrane (Fig. 1A). Together, these observations suggest that we can use either immunoperoxidase or immunogold labeling to localize Kv4.2 with this antibody. Although immunogold labeling has superior spatial localization compared to DAB, we decided to use DAB as our label of choice due to its higher sensitivity and lower noise level.

### **Ultrastructural Localization of Kv4.2 in the BLA**

Next, to test our hypothesis that stress causes alterations in the distribution of the voltage-gated A-type K<sup>+</sup> channel subunit Kv4.2 in the BLA, we examined two different time points: 1 and 6 days after the four-day stress protocol to determine the persistence of any observed change over a limited time period. However, to determine if there was stress-

induced redistribution, we first needed to determine the localization of Kv4.2 in the age-matched control animals. We examined the distribution of Kv4.2 in the control animals at both ages: 47 and 52 days (n= 6 and 5, respectively), which correspond to the ages of animals at the two different time points after completion of the stress protocol. This was done to determine if age was a confounding variable on the distribution of Kv4.2 in stressed animals at these time points.

In this preliminary analysis, we found that most of Kv4.2 immunoreactivity was in postsynaptic elements, i.e. spines (Fig. 2A) and dendritic shafts (Fig. 2B). This result is similar to previous *in vitro* and *in vivo* studies on the distribution of Kv4.2 (Sheng *et al.*, 1995; Hoffman *et al.*, 1997; Kim *et al.*, 2007; Menegola *et al.*, 2008; Jensen *et al.*, 2011). Additionally, although the majority of the Kv4.2-labeled profiles were comprised of dendritic shafts and spines, there were also a significant number of unlabeled dendritic shafts and spines in regions with extensive labeling. This observation was quantified by examining the data from the 11 control animals. From the images collected, we classified 220 to 358 labeled elements within the neuropil of the BLA from each control animal. We then calculated the percentage of labeled elements in five different components of the neuropil: spine, dendrite, terminal, axon, and glia. The data was then analyzed using a two-way ANOVA with factors of age and labeled profile. There was a significant main effect of labeled profile ( $F_{(4,45)}=487.493$ ,  $p<.0001$ ), with no significant main effect of age ( $F_{(4,45)}=0$ ,  $p>0.999$ ) or interaction between the age and labeled profiles ( $F_{(4,45)}=1.168$ ,  $p=0.3378$ ). Pooling the data from all the control animals, 13.0% of all immunoreactive profiles were spines, 66.6% dendritic shafts, 4.54% terminals, 4.64% axons, and 11.3% glial cells (Fig 2F). Post hoc Scheffe tests found significant differences between spines

and dendrites ( $p < 0.0001$ ), terminals ( $p = 0.0004$ ), and axons ( $p = 0.0005$ ), dendrites and terminals ( $p < 0.0001$ ), axons ( $p < 0.0001$ ), and glia ( $p < 0.0001$ ), terminals and glia ( $p = 0.0066$ ), and between axons and glia ( $p = 0.0002$ ) (Fig. 2F). However, no significant differences were found between spine and glia ( $p = 0.9172$ ) or terminals and axons ( $p > 0.9999$ ) (Fig. 2F). These data demonstrate that the vast majority of Kv4.2-labeled profiles in the BLA neuropil are postsynaptic elements, with almost 80% of all labeling seen in dendritic shafts and spines. A small amount of labeling was also found in presynaptic elements, i.e. terminals (Fig. 2C) and axons (Fig. 2D), and in glial cells (Fig. 2E), albeit much less when compared to postsynaptic structures.

Because previous studies have not described in detail Kv4.2 localization in presynaptic structures, we further characterized the labeled terminals in our sample to determine if they formed symmetric (i.e. putative inhibitory) or asymmetric (i.e. putative excitatory) synapses in the BLA. Of all the labeled terminals, 40.3% ( $n = 56$ ) made visible synapses in the single section examined. Of these, 5 made symmetric synapses onto dendritic shafts, while 51 made asymmetric synapses. The targets of these asymmetric synapses included 32 spines, 17 dendritic shafts and 2 that were unidentifiable in the single section analyzed. This suggests that presynaptic Kv4.2 is primarily positioned to modulate the function of putative excitatory, glutamatergic, synapses in the rat BLA.

### **Stress Induces an Increase in Kv4.2-Labeling in Dendritic Spines**

Having established the distribution of Kv4.2 in the BLA of normal animals, we next examined the effect of stress on its ultrastructural localization. We examined two different time points: 1 and 6 days after the four-day stress protocol ( $n = 6$  for both

groups), and compared them to all 11 control animals. From each stressed animal, we imaged and categorized 227 to 408 labeled elements within the neuropil of the BLA. We then calculated the percentage of labeled elements in five different components of the neuropil: spine, dendrite, terminal, axon, and glia. The distribution of Kv4.2 in the BLA for the three different groups is depicted in Figure 3. The data were then analyzed using a two-way ANOVA with factors of group (1-day post stress; 6-day post stress; control) and labeled profile. There was no significant main effect of group ( $F_{(4,100)}=0$ ,  $p>.999$ ), but there was a significant main effect of labeled profile ( $F_{(4,100)}=989.523$ ,  $p<.0001$ ), and a significant interaction between the groups and labeled profiles ( $F_{(8,100)}=3.632$ ,  $p=0.0010$ ).

Because the significant interaction between treatment and group indicates a treatment-induced effect in the frequency of label in one or more of the profile types, we followed this up with a secondary analysis to determine the profile types in which Kv4.2 localization was mainly affected. We conducted separate one-way ANOVAs split by profile. We found that stress significantly increased the percentage of Kv4.2-labeled spines ( $F_{(2,20)}=5.678$ ,  $p=0.0111$ ). Post hoc Scheffe tests found no significant difference between control and 1 day post stress ( $p=0.3022$ ) or between day 1 and day 6 post stress ( $p=0.3284$ ), but a significant increase in the percentage of Kv4.2-labeled spines between day 6 post stress animals and control ( $p=0.0119$ ). Stress also significantly reduced the percentage of labeled glia ( $F_{(2,20)}=3.919$ ,  $p=0.0366$ ); however, in our post hoc Scheffe tests, we found no significant differences were found between control and day 1 post stress ( $p=0.9934$ ), between control and day 6 post stress ( $p=0.0569$ ), nor between day 1 and day 6 post stress ( $p=0.0847$ ). No significant effect of stress was found for the rest of

the profiles: dendritic shafts ( $F_{(2,20)}=0.712$ ,  $p=0.5025$ ), terminals ( $F_{(2,20)}=3.363$ ,  $p=0.0551$ ), or axons ( $F_{(2,20)}=1.423$ ,  $p=0.2643$ ).

These findings suggest that stress results in an increased availability of Kv4.2 at excitatory synapses onto dendritic spines. In order to determine if this was a general effect at excitatory synapses throughout the BLA or restricted to axospinous synapses, we conducted a secondary analysis of the relative percentage of dendritic shafts that received asymmetric synaptic contacts between control and stressed animals (Fig. 4A). Because inhibitory interneurons are by far the most common target of asymmetric axo-dendritic synapses in the BLA, labeled dendrites with asymmetric synapses analyzed most likely belong to GABAergic interneurons (McGuire *et al.*, 1991). Therefore, examining such labeled postsynaptic dendritic shafts allowed us to analyze profiles of neuronal populations different from those that received axo-spinous glutamatergic afferents (i.e. presumed glutamatergic BLA projection neurons). Thus, we determined the fraction of labeled dendritic shafts that received asymmetric synaptic contacts in the plane of section and analyzed the data using a one-way ANOVA. We found that  $11.387 \pm 3.486\%$  of Kv4.2-labeled dendrites in control material received asymmetric synapses. Results from the ANOVA revealed no significant difference in the relative prevalence of these labeled dendritic profiles between normal and stressed animals ( $F_{(2,20)}=0.077$ ,  $p=0.9263$ ), thereby suggesting that the possible increase in Kv4.2 expression at excitatory synapses may be limited to axo-spinous synapses on BLA projection neurons (Fig. 4B).

#### **4. Discussion**

Using immunohistochemical techniques, we discovered that the bulk of voltage-gated A-type  $K^+$  channel subunit Kv4.2 immunoreactivity in the BLA is found primarily in postsynaptic neuronal elements (i.e. dendritic shafts and spines). Furthermore, our experiment demonstrated a stress-induced increase in the relative proportion of Kv4.2-labeled spines over other immunoreactive elements in the BLA. This result suggests that Kv4.2 might be involved in stress-mediated plasticity, modulating excitability at axo-spinous glutamatergic synapses in the BLA.

#### **Intracellular Localization of Kv4.2**

While the Kv4.2<sub>(209-225)</sub> antibody used in our experiment was predicted to bind to an extracellular epitope, we found that the labeling generated by this antibody in the rat BLA was intracellular using both immunoperoxidase and immunogold. In particular, we did not observe profiles labeled by gold along the external surface of their plasma membrane. This pattern of labeling is similar to that recently reported in another study using pre-embedding immunoperoxidase localization of the same antibody in the neurons of the intercalated cell clusters of Sprague-Dawley rats (Kaufmann *et al.*, 2012). These data suggest that the predicted extracellular binding target is inaccurate and that it is possible to use either immunoperoxidase or immunogold labeling to characterize the intracellular localization of Kv4.2 immunoreactivity in neuronal elements with this antibody. Possible reasons for this discrepancy in localization might be a change in the overall 3D protein structure of the channel subunit during a preparation step causing a relocation S1-S2 epitope to the intracellular surface, or that the predicted topology of

Kv4.2 is different *in vivo* (Kaufmann *et al.*, 2012). Another possible explanation is that most of Kv4.2 is found in internal stores in perfusion fixed material. Our data suggest that more studies need to be conducted to determine the exact conformation of Kv4.2 in plasma membranes *in vivo*.

### **Subcellular Distribution of Kv4.2 in the BLA**

While many *in vivo* studies of Kv4.2 have been conducted in other brain regions, particularly in the hippocampus, the subcellular localization of Kv4.2 in the BLA remains unknown. In the current study, we used immunohistochemical techniques at the electron microscopic level to determine the normal distribution of voltage-gated potassium channel subunit Kv4.2 in rat BLA neurons.

The results of this experiment demonstrate the pattern of Kv4.2 localization in the rat BLA and show that it does not vary across the (limited) age range used in our study. The majority of Kv4.2 immunoreactivity was observed in postsynaptic elements, with 13% of all immunoreactive profiles found in spines and 66.6% found in dendritic shafts. These results suggest that Kv4.2 regulates inputs into BLA neurons, which will be further discussed below.

Albeit scarce, immunoreactivity was also found in presynaptic elements (4.54% terminals; 4.64% axons) and 11.3% was found in glial cells (Fig. 2). This subcellular distribution differs from previous *in vitro* and *in vivo* studies of Kv4.2 localization that described Kv4.2 as being confined to postsynaptic elements (Sheng *et al.*, 1995; Hoffman *et al.*, 1997; Kim *et al.*, 2007; Menegola *et al.*, 2008; Jensen *et al.*, 2011). Kv4.2 was found mainly in putative excitatory terminals, with 91.1% of terminals having

asymmetric postsynaptic densities (PSD). Of these, 62.7% synapsed onto spines and 33.3% synapsed onto dendritic shafts. The results from this study suggest that Kv4.2 predominantly contributes to the modulation of presynaptic excitability and regulation of neurotransmitter release in glutamatergic terminals, which comprise the majority of excitatory synapses in the brain. Its presence in axons also suggests that it regulates the propagation of an AP (Sheng *et al.*, 1995). Further electrophysiological studies need to be conducted to determine the exact function of Kv4.2 in presynaptic elements as well as their function in glial cells.

### **Stress-Mediated Redistribution of Kv4.2**

In this study, we found a significant increase in the frequency with which Kv4.2-label was found in dendritic spines following stress. This was observed at the time point six-day after the stress exposure, but not at the one-day point. Additional analyses of the age-matched control animals suggest that the observed redistribution was not due to a relative change in composition in the neuropil of the BLA following stress or due to differences in the age of the animals over the two time points (Fig. 2F).

Previous studies have demonstrated that stress produces morphological changes in the brain. In several studies, chronic stress has been shown to increase spine density (Radley & Morrison, 2005; Vyas *et al.*, 2006; Qin *et al.*, 2011). This raises the possibility that the stress induced increase in Kv4.2 found in spines might be simply due to a stress-induced increase of the spine density, and not a redistribution of Kv4.2. However, Hubert *et al.*, found no significant change in the overall ratio of spines to dendrites in the BLA following our stress protocol in the same group of animals (Hubert *et al.*, in press).

In the same study, they also found no change in the membrane resistance ( $R_m$ ) of the principle neurons, suggesting no major atrophy or hypertrophy of dendritic branching (Hubert *et al.*, in press). Therefore, there is no detectable stress-induced morphological change in our animals. This suggests that the increase in the degree to which Kv4.2 label was found in spines is unlikely to be due simply to stress induced morphological changes.

Another possible explanation for the observed redistribution is pain-mediated plasticity. Current literature suggests that different types of pain induce redistribution of a variety of receptor subunits (Ikeda *et al.*, 2007; Ren & Neugebauer, 2010). However, in these studies, the animals were subject to more intense pain paradigms, such as arthritis and neuropathic pain models, than in the stress model used in our study. While we are unable to differentiate between the factors of pain and stress associated with our paradigm, footshock is a commonly used protocol to induce stress in rats. Furthermore, because the footshock intensity is relatively mild in our paradigm, pain-mediated translocation of Kv4.2 seems unlikely. Studies involving restraint or predatory stress paradigms should be conducted to confirm our result.

### **Functional Implications of Kv4.2 Redistribution**

Synaptic plasticity is a fundamental feature of learning mechanisms in the brain. There is accumulating evidence suggesting that synaptic plasticity is in part mediated by alterations to the expression levels of voltage-dependent  $\text{Na}^+$ ,  $\text{Ca}^{2+}$ ,  $\text{Cl}^-$  and  $\text{K}^+$  channels (Zhang & Linden, 2003; Marder & Goillard, 2006; Abraham, 2008). This modification of cell excitability is thought to be partially involved in the formation of memory (Zhang & Linden, 2003; Abraham, 2008).

The voltage-gated potassium channel is an integral membrane protein channel that modulates the electrophysiological properties of the neuron. Therefore, it is reasonable to postulate that the change in distribution of Kv4.2 observed in our experiment could impact the input-output function of the neuron. Previous studies of A-type  $K^+$  channels suggest that Kv4.2 is a modulator of bAPs and specific forms of synaptic plasticity. Activation of Kv4.2 in response to sufficient depolarization triggers a fast transient outward  $K^+$  current. Thus, The consequence of changes in Kv4.2 expression is an overall reduction in depolarization where Kv4.2 clusters. In doing so, Kv4.2 varies the action potential's duration and frequency. Studies have established that a reduction in functional Kv4.2 expression levels in hippocampal neurons augmented the amplitude and charge of mEPSCs (Hoffman *et al.*, 1997; Ramakers & Storm, 2002). In addition, application of HpTX3, a selective blocker of Kv4 channels reduces the threshold for LTP induction (Ramakers & Storm, 2002). Therefore, the increase in expression in dendritic spines could theoretically have the opposite effect: reducing the average amplitude and charge of mEPSCs.

Dendritic spines primarily receive excitatory inputs (Koch & Zador, 1993). Our data suggests that translocation of Kv4.2 mainly affects excitatory input in BLA neurons, as change was only observed in spines (Bourne & Harris, 2008). Secondary analysis of the neuropil compartment, demonstrates no change in the overall number of Kv4.2-labeled postsynaptic dendrites following our stress protocol (Fig. 4B), suggesting that this effect is only found in excitatory inputs synapsing onto spines and not in interneuron inputs synapsing onto dendritic shafts. Therefore, Kv4.2 seems to mainly modulate input directed at spiny excitatory cells in the BLA. In this region, Kv4.2 should reduce the

postsynaptic excitability, changing cellular response and output function. Further studies need to be conducted to determine the alterations Kv4.2 and  $I_A$  contribute to BLA cell function in normal and stressed animals.

There is extensive evidence that the BLA is involved in regulating the effects of stress on memory (McGaugh & Roozendaal, 2002). This involves alterations to the electrophysiological properties of principle neurons in the BLA. Stress can modulate the localization of signaling proteins such as AMPAR at the synaptic level, enhancing dendritic excitability, which in turn results in synaptic plasticity (Beattie *et al.*, 2000; Brown *et al.*, 2005; Kim *et al.*, 2007; Hubert *et al.*, in press). This enhancement of dendritic excitability is part of the pathology of anxiety disorders and higher amygdala basal activity levels are associated with stress and anxiety (Etkin & Wager, 2007; Rabinak *et al.*, 2011). Taking this into account, our results suggest that the increase in voltage-gated transient  $K^+$  channel expression in dendritic spines might be a compensatory mechanism in an attempt to reduce the aforementioned dendritic excitability that contributes to the manifestation of pathological stress behavior.

In a separate study conducted by Hubert *et al.*, redistribution of the AMPA subunit GluR1 was observed following unpredictable footshock stress (Hubert *et al.*, in press). Specifically, they found an increase in the ratio of GluR1-labeled spines to dendrites in 6-days post stress rats that persisted out to 14-days post stress, but was not evident in the 1-day post stress group (Hubert *et al.*, in press). This redistribution of GluR1 localization from dendritic shafts to spines has been shown to increase dendritic excitability and is thought to be a contributing factor to the expression of pathological stress behavior. Comparison of the similar timelines of GluR1 and Kv4.2 redistribution, it

seems that increase in localization of Kv4.2 in spines might be a roughly concurrent response to the increase in GluR1 in an attempt to decrease excitability in that region. Studies have shown the dynamic nature of Kv4.2 localization, with trafficking to and from the dendritic membranes occurring within minutes (Kim *et al.*, 2007). Therefore, taking into account the dynamic nature of Kv4.2 trafficking, and because the 6-day time course required for redistribution of GluR1 subunits, the redistribution of Kv4.2 could be a compensatory mechanism for the increase in dendritic excitability caused by the increase in GluR1 expression. Perhaps this compensatory mechanism is insufficient in patients with anxiety disorders, resulting in higher amygdala basal activity levels (Etkin & Wager, 2007; Rabinak *et al.*, 2011) and increased amygdala activity to neutral stimuli under non-threatening conditions (Brunetti *et al.*, 2010). If indeed the Kv4.2 response proves to be a homeostatic mechanism, this ion channel might be a suitable target for pharmacological intervention of chronic stress and anxiety disorders. If one is able to manipulate the redistribution of Kv4.2, inducing upregulation of Kv4.2 channels around excitatory input in the BLA, it might alleviate the manifestation of pathological stress behavior and prevent anxiety disorders like PTSD. Further studies need to be conducted to determine the exact association between Kv4.2 and GluR1, and the mechanics of stress-mediated Kv4.2 trafficking.

## References

- Abraham WC (2008). Metaplasticity: tuning synapses and networks for plasticity. *Nature Reviews Neuroscience* 9:387.
- Beattie EC, Carroll RC, Yu X, Morishita W, Yasuda H, von Zastrow M, Malenka RC (2000). Regulation of AMPA receptor endocytosis by a signaling mechanism shared with LTD. *Nat Neurosci.* 3(12):1291-300.
- Birnbaum SG, Varga AW, Yuan LL, Anderson AE, Sweatt JD, Schrader LA (2004). Structure and Function of Kv4-Family Transient Potassium Channels. *Physiol Rev* 84:803-833.
- Bourne JN, Harris KM (2008). Balancing structure and function at hippocampal dendritic spines. *Annu Rev Neurosci* 31:47-67.
- Brown TC, Tran IC, Backos DS, Esteban JA (2005). NMDA receptor-dependent activation of the small GTPase Rab5 drives the removal of synaptic AMPA receptors during hippocampal LTD. *Neuron* 6;45(1):81-94.
- Brunetti M, Sepede G, Mingoia G, Catani C, Ferretti A, Merla A, Del Gratta C, Romani GL, Babiloni C (2010). Elevated response of human amygdala to neutral stimuli in mild post traumatic stress disorder: neural correlates of generalized emotional response. *Neuroscience* 168(3):670-9.
- Chen X, Yuan LL, Zhao C, Birnbaum SG, Frick A, Jung WE, Schwarz TL, Sweatt JD, Johnston D (2006). Deletion of Kv4.2 genes eliminates dendritic A-type K<sup>+</sup> current and enhances induction of long-term potentiation in hippocampal CA1 pyramidal neurons. *The Journal of Neuroscience* 26(47):12143-12151.
- Davis M (1992). The role of the amygdala in fear and anxiety. *Annual Review of Neuroscience* 15(1):353-375.
- Davis M, Rainnie D, Cassell M (1994). Neurotransmission in the rat amygdala related to fear and anxiety. *Trends in Neuroscience* 17:208-214.
- Etkin A, Wager TD (2007). Functional neuroimaging of anxiety: a meta-analysis of emotional processing in PTSD, social anxiety disorder, and specific phobia. *The American Journal of Psychiatry* 164:1477-1488.
- Hazra R, Guo JD, Dabrowska J, Rainnie DG (2012). Differential distribution of serotonin receptor subtypes in BNST(ALG) neurons: Modulation by unpredictable shock stress. *Neuroscience*.

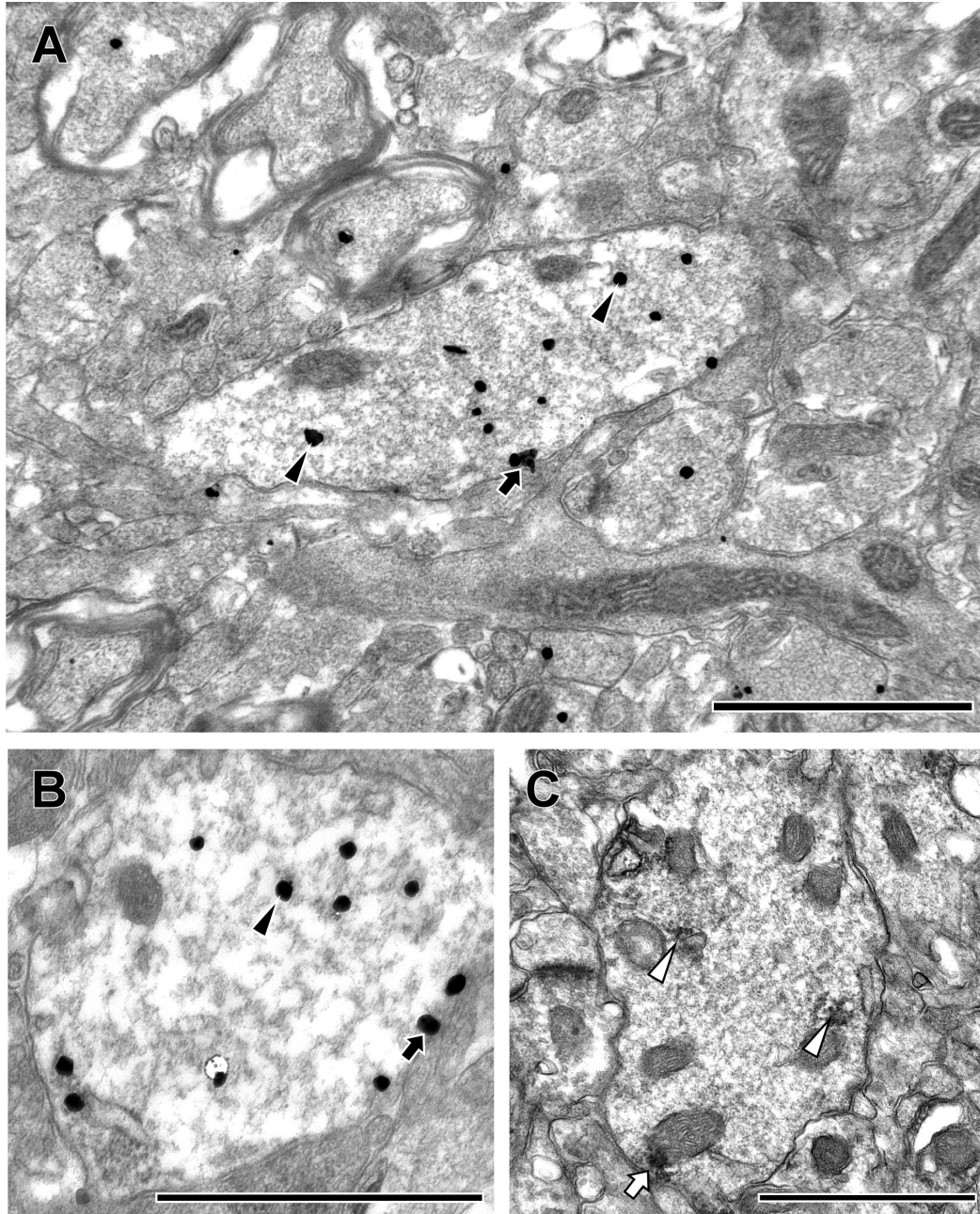
- Helmstetter FJ, Bellgowan PS. 1994. Effects of muscimol applied to the basolateral amygdala on acquisition and expression of contextual fear conditioning in rats. *Behavioral Neuroscience* 108:1005–9.
- Hoffman DA, Magee JC, Colbert CM, Johnson D (1997). K<sup>+</sup> channel regulation of signal propagation in dendrites of hippocampal pyramidal neurons. *Nature* 387:869-875.
- Hubert GW, Li C, Rainnie DG, Muly EC (in press). Effects of Stress on AMPA Receptor Distribution and Function in the Basolateral Amygdala. *Brain Struct Funct* [Epub ahead of print].
- Ikeda R, Takahashi Y, Inoue K, Kato F (2007). NMDA receptor-independent synaptic plasticity in the central amygdala in the rat model of neuropathic pain. *Pain* 127(1-2):161-72.
- Jensen CS, Rasmussen HB, Misonou H (2011). Neuronal trafficking of voltage-gated potassium channels. *Molecular and Cellular Neuroscience* 48:288-297.
- Kaufmann WA, Matsui K, Jeromin A, Nerbonne JM, Ferraguti F (2012). Kv4.2 potassium channels segregate to extrasynaptic domains and influence intrasynaptic NMDA receptor NR2B subunit expression. *Brain Struct Funct*. [Epub ahead of print].
- Kim JH, Jung SC, Clemens AM, Petralia RS, Hoffman DA (2007). Regulation of Dendritic Excitability by Activity-Dependent Trafficking of the A-Type K<sup>+</sup> Channel Subunit Kv4.2 in Hippocampal Neurons. *Neuron* 54:933-947.
- Koch C, Zador A (1993). The Function of Dendritic Spines: Devices Subserving Biochemical Rather than Electrical Compartmentalization. *The Journal of Neuroscience* 13(2):413-422.
- Rather Than Electrical Compartmentalization
- Linnman C, Zeffiro TA, Pitman RK, Milad MR (2011). An fMRI study of unconditioned responses in post-traumatic stress disorder. *Biol Mood Anxiety Disord* 1:8.
- Lockridge A, Su J, Yuan LL (2010). Abnormal 5-HT modulation of stress behaviors in the Kv4.2 knockout mouse. *Neuroscience* 170(4):1086-97.
- Marder E, Goaillard JM (2006). Variability, compensation and homeostasis in neuron and network function. *Nature Reviews Neuroscience* 7:563-574.
- Maren S, Fanselow MS (1996). The Amygdala Minireview and Fear Conditioning: Has the Nut Been Cracked? *Neuron* 16:237-240.

- Maren S, Aharonov G, Stote DL, Fanselow MS (1996). N-methyl-D-aspartate receptors in the basolateral amygdala are required for both acquisition and expression of conditional fear in rats. *Behav Neurosci*. 110(6):1365-74.
- McDonald AJ (1998). Cortical pathways to the mammalian amygdala. *Prog Neurobiol* 55:257-332.
- McGaugh JL, Roozendaal B (2002). Role of adrenal stress hormones in forming lasting memories in the brain. *Curr Opin Neurobiol* 12:205-210.
- McGuire BA, Gilbert CD, Rivlin PK, Wiesel TN (1991). Targets of horizontal connections in macaque primary visual cortex. *The Journal of Comparative Neurology* 305(3):370-392.
- Menegola M, Misonou H, Vacher H, Trimmer JS (2008). Dendritic A-type potassium channel subunit expression in CA1 hippocampal interneurons. *Neuroscience* 154:953-964.
- Muller J, Corodimas KP, Fridel Z, LeDoux JE (1997). Functional inactivation of the lateral and basal nuclei of the amygdala by muscimol infusion prevents fear conditioning to an explicit CS and to contextual stimuli. *Behavioral Neuroscience* 111:683-91.
- Muly EC, Maddox M, Khan ZU (2010). Distribution of D1 and D5 dopamine receptors in the primate nucleus accumbens. *Neuroscience* 169(4):1557-1566.
- Muly EC, Maddox M, Smith Y (2003). Distribution of mGluR1alpha and mGluR5 immunolabeling in primate prefrontal cortex. *The Journal of Comparative Neurology* 467(4):521-535.
- Nader K, Majidishad P, Amorapanth P, LeDoux JE (2001) Damage to the lateral and central, but not other, amygdaloid nuclei prevents acquisition of auditory fear conditioning. *Learn Mem* 8:156-163.
- Peters A, Palay S, Webster H (1991). *The Fine Structure of the Nervous System*. New York: Oxford Press.
- Purves D, Augustine G, Fitzpatrick D, Hall WC, LaMantia AS, McNamara JO, White LE (2008). *Neuroscience* (4th ed.). Sunderland, MA: Sinauer Associates.
- Qin M, Xia Z, Huang T, Smith CB (2011). Effects of chronic immobilization stress on anxiety-like behavior and basolateral amygdala morphology in Fmr1 knockout mice. *Neuroscience* 194:282-290.
- Rabinak CA, Angstadt M, Welsh RC, Kenndy AE, Lyubkin M, Martis B, Phan KL (2011). Altered amygdala resting-state functional connectivity in post-traumatic stress disorder. *Front Psychiatry* 2:62.

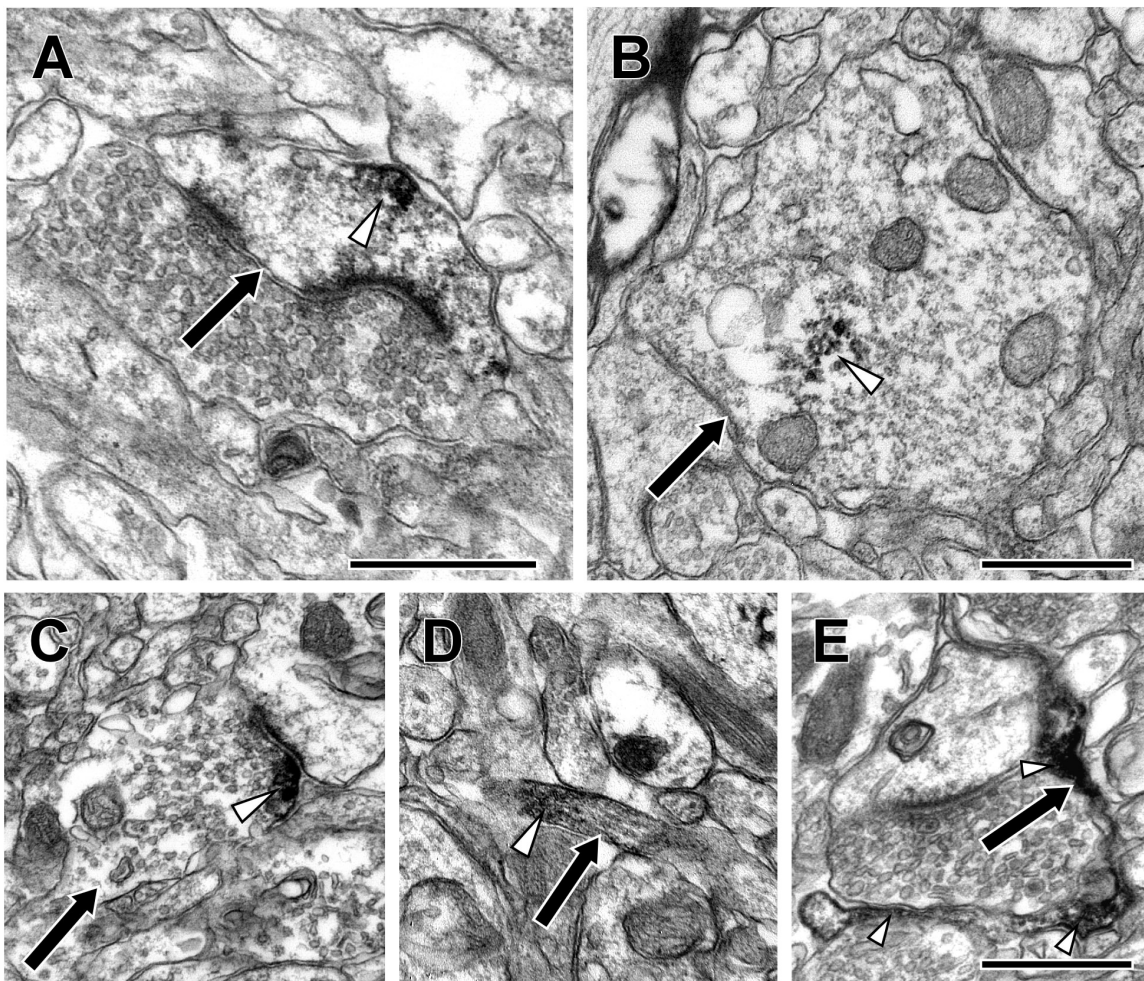
- Rabinak CA, Angstadt M, Welsh RC, Kenndy AE, Lyubkin M, Martis B, Phan KL (2011). Altered amygdala resting-state functional connectivity in post-traumatic stress disorder. *Front Psychiatry* 2:62.
- Radley JJ, Morrison JH (2005). Repeated stress and structural plasticity in the brain. *Ageing Research Review* 4(2):271-287.
- Ramakers GM, Storm JF (2002). A postsynaptic transient K<sup>+</sup> current modulated by arachidonic acid regulates synaptic integration and threshold for LTP induction in hippocampal pyramidal cells. *Proc Natl Acad Sci U S A* 99(15):10144–10149.
- Rainnie DG, Hazra R, Dabrowska J, Guo JD, Li CC, Muly EC (Submitted). Distribution and functional expression of Kv4 family  $\alpha$  subunits and associated KChIP  $\beta$  subunits in the bed nucleus of the stria terminalis. *The Journal of Comparative Neurology*.
- Ramakers GM, Storm JF (2002). A postsynaptic transient K(+) current modulated by arachidonic acid regulates synaptic integration and threshold for LTP induction in hippocampal pyramidal cells. *Proc Natl Acad Sci U S A*. 99(15):10144-9.
- Rauch SL, Shin LM (1997). Functional neuroimaging studies in posttraumatic stress disorder. *Annals of the New York Academy of Sciences* 821:83-98.
- Rauch SL, Shin LM, Phelps EA (2006). Neurocircuitry models of posttraumatic stress disorder and extinction: Human neuroimaging research—past, present, and future. *Biol Psychiatry* 60:376-382.
- Ren W, Neugebauer V (2010). Pain-related increase of excitatory transmission and decrease of inhibitory transmission in the central nucleus of the amygdala are mediated by mGluR1. *Molecular Pain* 6:93.
- Reynolds E (1963). The use of lead citrate at high pH as an electron opaque stain in electron microscopy. *J Cell Biol* 17: 208–212.
- Sheng M, Jan YN, Jan L (1995). The molecular organization of voltage-dependent K<sup>+</sup> channels in vivo. *Progress in Brain Research* 105: 87-93.
- Shin LM, Liberzon I (2010). The neurocircuitry of fear, stress, and anxiety disorders. *Neuropsychopharmacology* 35:169-191.
- Shors TJ (2001). Acute stress rapidly and persistently enhances memory formation in the male rat. *Neurobiol Learn Mem* 75:10-29.
- Trimmer JS, Rhodes KJ (2004). Localization of voltage-gated ion channels in mammalian brain. *Annu Rev Physiol* 66:477-519.

- Vyas A, Jadhav S, Chattarji S (2006). Prolonged behavioral stress enhances synaptic connectivity in the basolateral amygdala. *Neuroscience* 143(2):387-393.
- Walker DL, Davis M (2008) Role of the extended amygdala in short-duration versus sustained fear: A tribute to Dr. Lennard Heimer. *Brain Struct Funct* 213:29-42.
- Zhang W, Linden DJ (2003). The other side of the engram: experience-driven changes in neuronal intrinsic excitability. *Nature Reviews Neuroscience* 4:885-900.

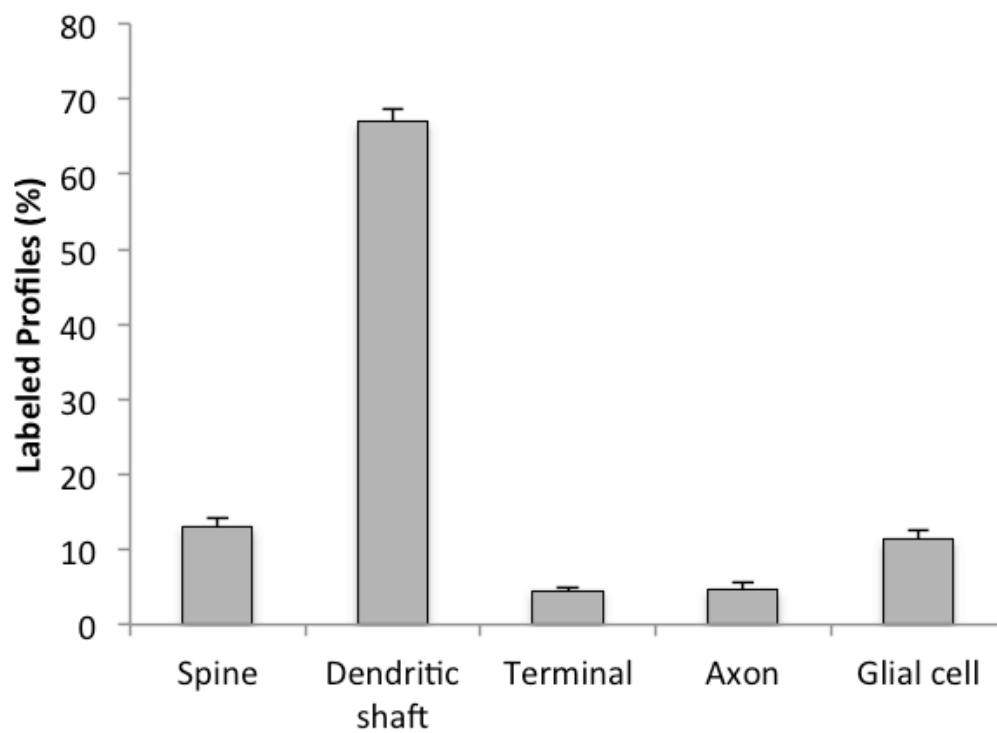
## Figure Legends



**Figure 1.** Intracellular localization of Kv4.2. **A-C:** Electron micrographs of Kv4.2 immunoreactive dendritic shafts in the rat BLA. **(A-B)** Immunogold. **(C)** Immunoperoxidase. Black arrowheads indicate intracellular immunogold label; black arrows indicate plasma membrane immunogold label; white arrowheads indicate intracellular DAB label; and white arrows indicate plasma membrane DAB label. Note that there are non-labeled profiles intermingled with the labeled ones. Localization pattern of Kv4.2 using immunogold and immunoperoxidase is similar, with it being found both intracellularly and on the inner portion of the plasma membrane. Scale bar is 1  $\mu$ m.



**Figure 2.** Kv4.2 immunoreactivity in the BLA from the control animals. **A-E:** Electron micrographs of Kv4.2 immunoreactivity in the BLA. Immunoperoxidase staining of 55-nm ultrathin BLA sections with anti-Kv4.2 monoclonal antibodies. The vast majority of Kv4.2-labeled profiles in the BLA neuropil are in presynaptic elements, with almost 80% of all labeling seen in dendritic shafts and spines. White arrowheads indicate DAB label. **(A)** Arrows indicates Kv4.2-immunoreactive spines. **(B)** Arrow indicates Kv4.2-immunoreactive dendritic shafts. **(C)** Arrow indicates Kv4.2-immunoreactive terminals. **(D)** Arrow indicates Kv4.2-immunoreactive axons. **(E)** Arrow indicates Kv4.2-immunoreactive glial processes. Scale bar is 1 $\mu$ m.

**F**

**Figure 2. (F)** Bar chart of the combined distribution of Kv4.2 immunoreactivity in different types of neuronal elements. As age does not seem to have an effect on the distribution of Kv4.2 in the BLA, the data from control animals (1-day; 6-days) were pooled together. Bars indicate SEM (n=11).

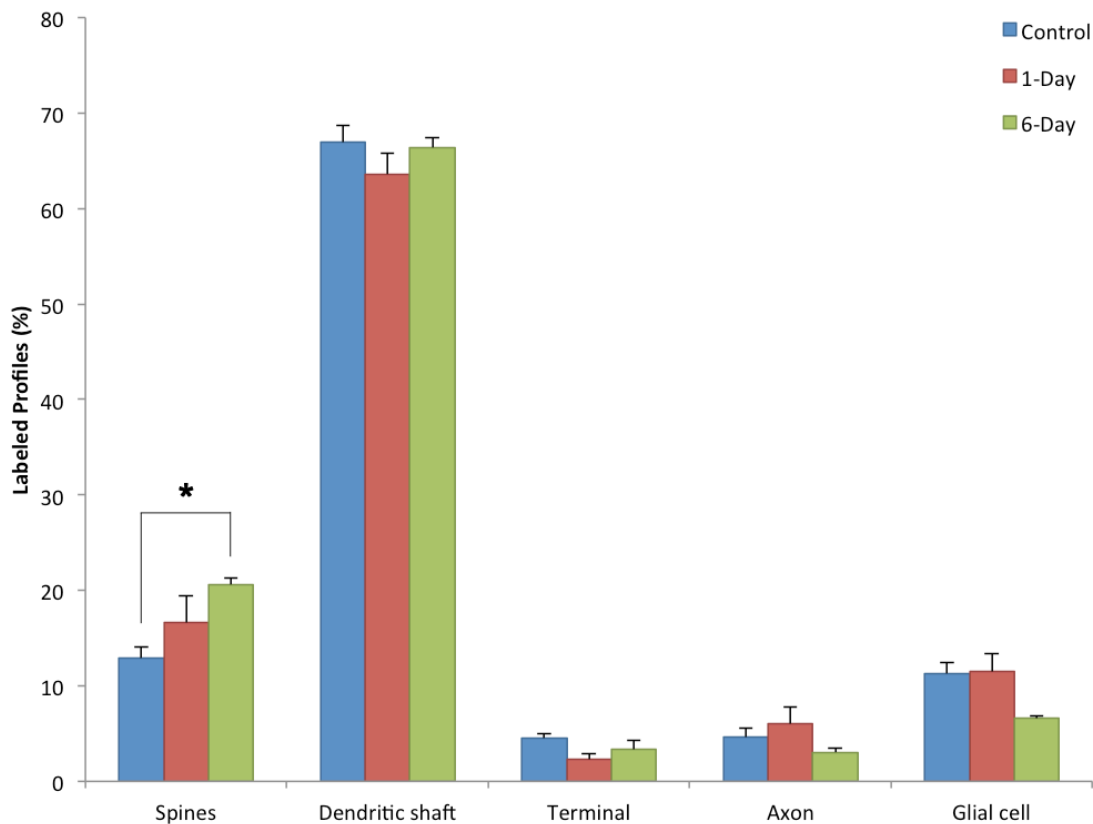
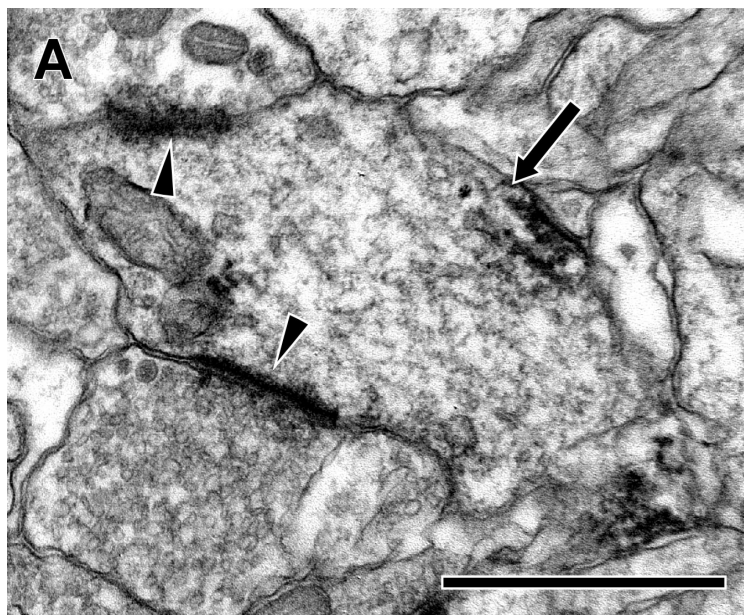


**Figure 3.** Effect of stress on Kv4.2 distribution. This bar chart represents the distribution of Kv4.2 immunoreactivity in different types of neuronal elements, in control, 1-day post stress, and 6-day post stress animals. Kv4.2 is primarily located in the postsynaptic elements (dendritic shafts and spines) with very little observed in presynaptic elements or glia. Bars indicate SEM (n=23). Asterisks indicate a significance level of  $p < 0.05$ .



**B**

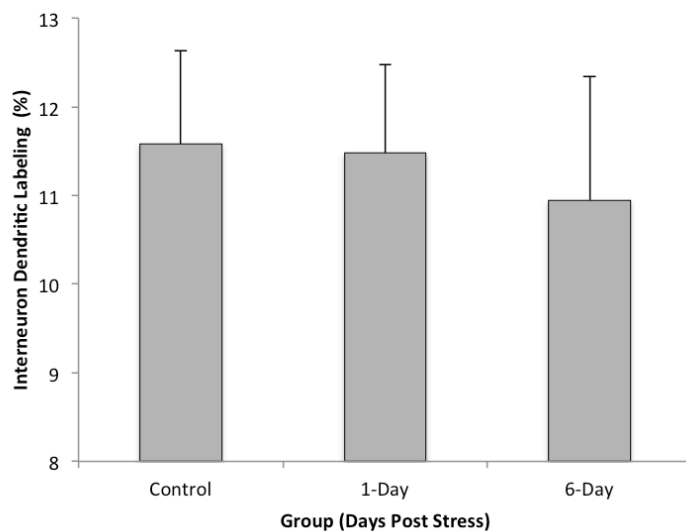


**Figure 4.** No significant reduction in putative interneuron dendritic labeling in the BLA between control and stressed animals. **(A)** Electron micrograph of a Kv4.2-immunoreactive dendrite that receives multiple asymmetric synaptic inputs (arrowheads) in the BLA. Arrow indicates Kv4.2-labeled synaptic dendrite. Arrowheads indicate asymmetric synapse. Scale bar is 1 $\mu$ m. **(B)** Summarized percentage of Kv4.2-labeled asymmetric synaptic contacts onto dendrites for each treatment. The percentage of Kv4.2-labeled synaptic dendrites was calculated in control animals and in both groups of stressed animals (1- and 6-day post stress groups). Inhibitory interneurons receive asymmetric synaptic contacts on dendritic shafts. There was no significant effect of time post stress on the relative percentage of Kv4.2-immunoreactive dendrites with asymmetric synaptic inputs (i.e. from putative interneurons) ( $F_{(2,20)}=0.077$ ,  $p=0.9263$ ). Increase in Kv4.2 is limited to the dendritic spines of excitatory projection neurons (n=23).